

# Strength prediction in composites with stress concentrations: classical Weibull and critical failure volume methods with micromechanical considerations

E. V. Iarve · D. Mollenhauer · T. J. Whitney · R. Kim

Published online: 8 August 2006  
© Springer Science+Business Media, LLC 2006

**Abstract** Application of Weibull statistics to tensile strength prediction in laminated composites with open holes is revisited. Quasi-isotropic carbon fiber laminates with two stacking sequences  $[45/0/-45/90]_s$  and  $[0/45/90/-45]_s$  with three different hole sizes of 2.54, 6.35 and 12.7 mm were considered for analysis and experimental examination. The first laminate showed 20% lower strength for smaller and 10% for the larger hole sizes. A novel critical failure volume (CFV) method with minimum scaling length constraint as well as the traditional Weibull integral method were applied. The strength prediction was based on the state of stress in the  $0^\circ$  ply by taking into account the redistribution of stress due to matrix damage in the form of splitting, delamination and matrix cracking of off axis plies. The state of matrix damage precipitating failure was recorded by using X-radiography and examined by a sectioning technique. The measured extent of damage was then included in a 3D stress analysis procedure by using a mesh independent crack modeling method to account for fiber direction stress redistribution. The CFV method gave results within one standard deviation from experimentally observed strength values for both laminates and all three hole sizes. The Weibull integral method underpredicted the strength in all cases from as much as 20–30% for smaller hole sizes to 8% for the large holes. The accuracy of failure predictions using CFV is attributed to the introduction of a minimum scaling length. This length

has a physical meaning of the width of a process zone of formation of fiber macro-crack as a result of single fiber break interaction. Direct measurement or rigorous evaluation of this parameter is, however, difficult. Consistent with referenced micromechanical studies, its value was assigned equal to six times the Rosen's ineffective length.

## Introduction

The strength prediction of composites with stress concentrations is concerned with material response in small highly stressed volumes. Direct evaluation of material strength in such areas is difficult to achieve in practice. On the other hand, the ability of such small regions to sustain loads exceeding the average strength measured on uniformly loaded coupons, e.g. ASTM standard for axial strength testing in unidirectional composites [1], is the foundation of the long standing Whitney–Nuismer point and average stress failure criteria [2]. These criteria postulate that the failure of a composite with stress concentrations occurs when a finite size volume near the stress concentration is loaded at or above the average strength measured on standard test coupons without stress concentrators. The size of this volume constitutes an additional material property. These two parameter criteria along with a fracture mechanics based criterion [3] provide the foundation of the industrial composite bolted joint design tools that are in service today. Two types of stress concentrations in the form of through the laminate thickness cracks and holes were considered in the original studies [2–5]. The characteristic dimensions in the point and average stress failure criteria were established to be 1.016 mm and 3.81 mm, respectively. Obtained for glass/epoxy Scotchply, these

E. V. Iarve (✉) · T. J. Whitney · R. Kim  
University of Dayton Research Institute, 300 College Park Ave.,  
Dayton, OH 45469-0168, USA  
e-mail: endel.iarve@wpafb.af.mil

D. Mollenhauer  
U.S. Air Force Research Laboratory, AFRL/MLBC,  
Wright-Patterson AFB, OH 45433-7750, USA

dimensions were also shown to adequately describe the effect of strength increase with reduction in size of the crack/hole in T300/5208 graphite epoxy laminates. It was noticed however, in [4] that for some laminates the accuracy of predictions with the cited characteristic dimension values was unsatisfactory. While proving accurate and efficient for capturing the notch size effect on strength within a given laminate family, these dimensions have not found clear physical interpretation and appear not to represent a fundamental material property. Indeed, in-depth studies of composite laminates with through the thickness cracks and sharp notches by Kortshot and Beaumont [6] revealed complex failure mechanism. According to [6], matrix cracking in the form of splitting as well as accompanying delamination lead to significant reduction and dispersion of the stress concentration in the fiber direction as compared to a crack type stress singularity. The Weibull scaling based integral approach was then applied to non-uniform fiber direction stress distribution to predict the average failure load.

The present paper will attempt such an approach for composite laminates with open holes. The emphasis will be on evaluation of the limits of the applicability of the traditional Weibull integral based fiber direction strength scaling. We shall experimentally obtain the extent of matrix damage at loads close to failure in quasi-isotropic laminates with two stacking sequences:  $[45/0/-45/90]_s$  and  $[0/45/90/-45]_s$ . The matrix cracking and delaminations observed will then be modeled by using a mesh-independent damage modeling technique [7–9]. Weibull scaling of fiber direction strength will be applied to strength prediction in the  $0^\circ$  ply and compared to experiments. A critical element of analysis involving statistical distributions of strength is the quality of the strength data used for analysis. A review of research devoted to investigation of composite strength scaling under various loading conditions was carried out by Wisnom [10]. While the trend of strength increase with decreasing specimen size was apparent with regard to fiber direction tensile failure, there was no methodology for reliable measurement of its Weibull parameters. Such methodology was recently developed by Wisnom et al. [11] and experimental data obtained for an IM7/8552 material. The material system utilized in our experiments was IM7/5250-4. It was assumed that these two material systems possess similar fiber direction properties at room temperature and thus Weibull parameters from [11] were used in the present study.

Application of Weibull based strength scaling approach to strength prediction of composites with open holes was pioneered by Wu [12], Wetherhold and Whitney [13], and Wetherhold [14]. References [12, 13] addressed the effect of the hole size on the strength of composite laminates and showed qualitative agreement with experimental data. The

details of the analyses performed in [12] are not revealed whereas a simplified one dimensional Weibull integration along the tensile failure plane perpendicular to loading and passing through the center of the hole was used in [13]. In the follow on research, Wetherhold [14] considers reliability of open hole laminates under multiaxial loading by using a Lekhnitskii solution to define the two dimensional stress field. A particularly interesting aspect of this work is that it develops a failure localization methodology, which is based on evaluation of reliability (1 minus probability of failure) of nonoverlapping subvolumes by subdividing the laminate with the hole into regions similar to finite element subdivision. In this case, however, volume discretization was performed for Weibull integral calculation only. The Weibull integral was calculated for each subregion to evaluate its reliability and then this reliability was divided by the volume of that region. It was shown that this approach qualitatively predicts the localization of the failure region near the stress concentration for material with low variability and its dispersion for materials with high strength variability. However, the proposed quantity, the “reliability density,” may not be suitable for quantitative evaluation of the most likely failure region, because it appears to be dependent on the subdivision. Thus analyzing the same stress field with two subdivision where one is a refinement of another, the “reliability density” of every volume of refined subdivision will be higher than that calculated for the first subdivision. In the limit of infinite subdivision refinement the “reliability density” will also infinitely grow.

A method for identifying the critical failure volume (CFV), i.e. the most likely failure volume, was recently proposed in [15]. The key difference between the CFV method and Weibull integral method is that the former evaluates the probability of loss of load carrying capacity of a finite volume, and not that of its infinitesimal subdomain, and thereby is not derived from the weakest link concept. The quantitative definition of the CFV in the problems with stress concentrations is especially important in heterogeneous materials such as composites. As shown in [15], the CFV size can be below the limits of applicability of Weibull stress scaling obtained on a macro-specimen scale and require micromechanical, i.e. fiber/matrix level, considerations. Experimentation is carried out in the present work to evaluate this effect.

## Experimental

Coupons cut from quasi-isotropic IM7/5250-4 laminates with two different stacking sequences were subjected to quasi-static tensile loading. The stacking sequences were  $[45/0/-45/90]_s$  and  $[0/45/90/-45]_s$ . Nominal thickness of all

specimens was 1.11 mm. Three different hole sizes, 2.54, 6.35 and 12.7 mm in diameter, were drilled by using diamond drill bits. Sets of 18 specimens were tensile tested for each of the two smaller hole sizes for each laminate to obtain the tensile strength. The specimen width was 25.4 mm and 38.1 mm, respectively. Three  $[45/0/-45/90]_s$  specimens were tensile tested with the hole size 12.7 mm (width 76.2 mm). Due to unforeseen difficulties only one data point was obtained for the large hole size in the  $[0/45/90/-45]_s$  laminate. Such inconsistency in reliability of data is partially due to the fact that only the two smaller hole sizes were planned for investigation initially. However, due to some material surplus the data for larger hole size were also obtained and included.

The laminate with outside  $0^\circ$  plies showed significantly higher tensile strength for all hole sizes. Such difference was attributed to fiber direction stress relaxation due to matrix cracking in the form of splitting and delamination [9] affecting this stacking sequence. The extent of matrix damage in the present study was obtained by using additional specimens, which were tensile loaded to loads approximately 83–91% of the tensile failure loads measured previously. These specimens were then X-rayed and two of them sectioned. In the case of the 12.7 mm hole diameter specimen with  $[0/45/90/-45]_s$  stacking sequence the tensile strength reported is the strength of the specimen X-rayed.

Initial drilling damage was evaluated by X-raying the specimens before loading. Some matrix cracking and delamination was observed in the specimens with 2.54 mm hole diameter. However, the damage appeared to be located in the areas away from those exposed to overstress as shown in the Fig. 1. The loading direction corresponds to the  $x$ -direction. The laminates with the other two hole sizes revealed no drilling damage visible on X-ray.

An important aspect of the present approach is to evaluate and model the main features of the state of matrix damage preceding the fiber failure. Figure 2 displays die penetrant enhanced X-ray images of matrix cracking and delamination precipitating the final specimen failure for all specimens except the 12.7 mm  $[45/0/-45/90]_s$  which was unavailable. Table 1 shows the load values at which these images were taken and in parentheses the percentage of the

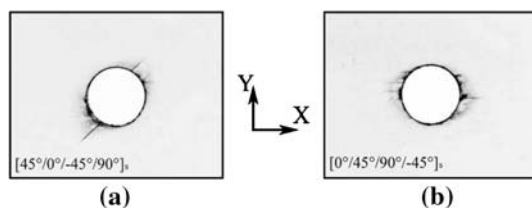


**Fig. 1** X-ray image of drilling damage in laminates with 2.54 mm holes, (a)  $[45/0/-45/90]_s$  laminate and (b)  $[0/45/90/-45]_s$  laminates. Note: no damage visible in larger hole sizes

final failure load. The tensile strength values are given in Table 3 and will be discussed subsequently. The damage observed in all images consists of matrix cracking and delaminations. Drastically different size of the near hole region affected by matrix damage can be seen for the two laminates. In the case of the  $[45/0/-45/90]_s$  laminate the size of splits in the  $0^\circ$  ply appears to scale with the hole size and equals approximately one diameter. In the  $[0/45/90/-45]_s$  laminate, the splits in the zero degree ply are longer than the two smallest hole diameters. In fact, it appears that these splits grow to approximately the same length regardless of the hole size. All images contain significant amount of matrix cracking in  $+45$  and  $-45$  plies. Ref. [8] considered the influence of matrix cracks in the off-axis plies on the stress redistribution in the load carrying  $0^\circ$  ply and showed that such influence is small in comparison to the effects of splitting in the  $0^\circ$  ply itself. Thus in the present work, we will only model the splitting of  $0^\circ$  plies, any delamination on their interfaces and the cracks in the adjacent plies such as the  $45^\circ$  in the  $[0/45/90/-45]_s$  laminate and the  $45^\circ$  and  $-45^\circ$  cracks in the  $[45/0/-45/90]_s$  laminate. A significant effect on the fiber direction stress is played by the delamination, which separates the  $0^\circ$  ply from the rest of the laminate. In the case of  $[45/0/-45/90]_s$  laminates, Fig. 2a, c the X-ray does not indicate suspect delamination areas. In the case of the  $[0/45/90/-45]_s$  laminate, Fig. 2b, d, f, a darker shadow is present in the stress concentration area ( $\theta = 90^\circ$ ) for the two larger hole sizes, whereas no shadow can be seen for the hole size of 2.54 mm. Specimens with hole diameter 2.54 mm and 6.35 mm were sectioned along the symmetry line perpendicular to loading direction. Microscopic inspection showed no delaminations present in the stress concentration area on the  $0^\circ/45^\circ$  ply interface. The shadow on the X-rays corresponded to a delamination between the  $90^\circ$  and  $-45^\circ$  plies. However, the dark shadows in the small regions between the splits and the hole edge were found to correspond to delaminations on the  $0^\circ/45^\circ$  interface. The cross sections of the 2.54 mm specimen in vertical planes just off the centerline of the specimen are shown on Fig. 3. The delamination is clearly seen inbound (toward the hole edge) extending up until the split. Figure 4 shows the schematics of the damage pattern modeled in each laminate. The split and crack length in all cases is shown in Table 2. The delamination contours were modeled as ellipses truncated by the splits in the  $0^\circ$  ply. The lengths of the half axes of these ellipses also are shown in Table 2. All damage was modeled anti-symmetrically about the horizontal centerline of the specimen.

### Stress analysis and $\nu(q)$ function calculation

Consider a rectangular orthotropic plate containing a circular hole having a diameter  $D$ , as shown in Fig. 5. The

**Fig. 2** X-ray images of matrix damage state for 2.54 mm hole (a) [45/0/-45/90]<sub>s</sub> and (b) [0/45/-45/90]<sub>s</sub>, 6.35 mm hole (c) [45/0/-45/90]<sub>s</sub> and (d) [0/45/-45/90]<sub>s</sub>, and 12.7 mm hole (e) [45/0/-45/90]<sub>s</sub> (unavailable) and (f) [0/45/-45/90]<sub>s</sub>. Load applied in the x-direction

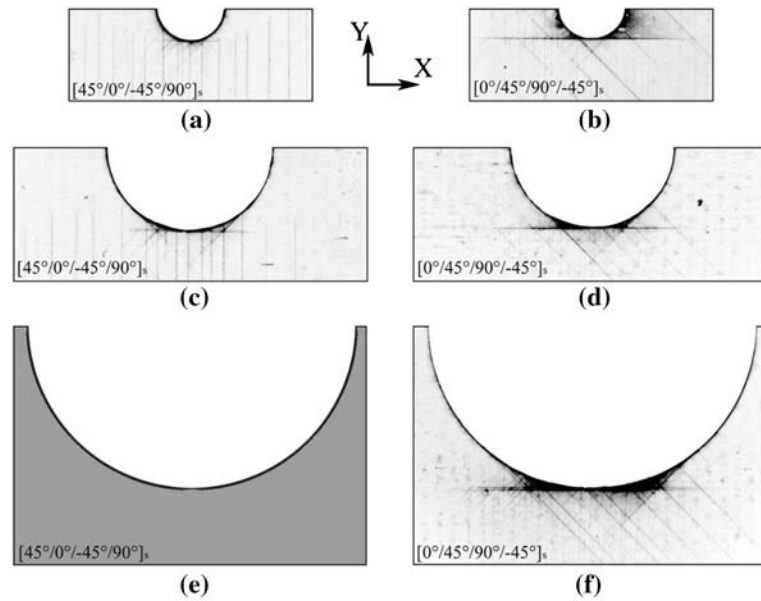


**Table 1** Load values at which the X-ray images of matrix damage were taken

| Hole diameter | X-ray image loads in MPa and % of failure stress |                            |
|---------------|--|----------------------------|
|               | [45/0/-45/90] <sub>s</sub>                       | [0/45/90/-45] <sub>s</sub> |
| 2.54 mm       | 507.9 (89%)                                      | 616.3 (91%)                |
| 6.35 mm       | 414.6 (88%)                                      | 507.9 (90%)                |
| 12.7 mm       | N/A  | 344.7 (83%)                |

plate consists of  $N$  plies of total thickness  $H$  in the  $z$ -direction and has a length  $L$  in the  $x$ -direction and width  $A$  in the  $y$ -direction. The following displacement boundary conditions were applied to the specimen

$$\begin{aligned} -u_x(0, y, z) &= u_x(L, y, z) = \varepsilon_0 L / 2 \\ u_y(0, 0, 0) &= u_z(x, y, 0) = 0. \end{aligned} \tag{1}$$

Traction-free boundary conditions are present on all other surfaces. The dimensionless loading parameter  $\varepsilon_0$  corresponds to relative elongation of the specimen. The  $z$ -direction displacement component on the bottom surface is constrained due to the symmetric lay-up of the laminates considered, which allows one to model only half of the specimen. The constitutive relations of each ply are as follows:

$$\sigma_{ij} = C_{ijkl}^p (\varepsilon_{kl} - \alpha_{kl}^p \Delta T), \quad i = 1, \dots, N,$$

where  $C_{ijkl}^p$  and  $\alpha_{kl}^p$  are elastic moduli and thermal expansion coefficients of the  $p$ th orthotropic ply, and  $\Delta T$  is the temperature change. The average applied traction is calculated as

$$\sigma_0 = \int_{y,z} \sigma_{xx}(0, y, z) dy dz. \tag{2}$$

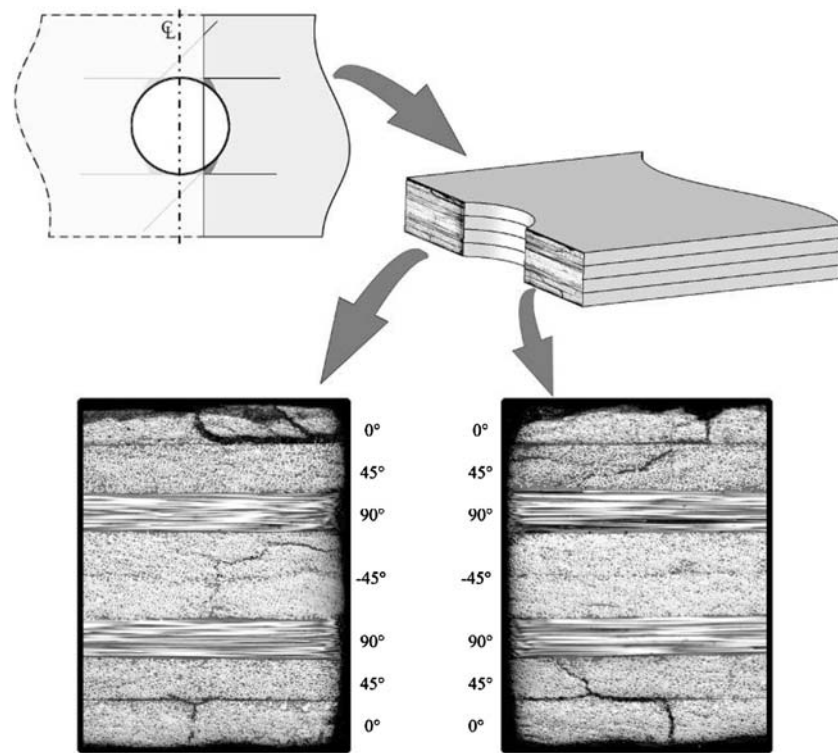
A three-dimensional displacement approximation is built by using the tensor product of one-dimensional approximations. Considering an elementary cube  $[0, 1]^3$  in local  $x_1, x_2, x_3$  coordinate system the 3-D displacement approximation can be written as

$$\mathbf{u}(x_1 x_2 x_3) = \sum_i \sum_j \sum_k X_i(x_1) Y_j(x_2) Z_k(x_3) \mathbf{U}_{ijk}, \tag{3}$$

where  $\mathbf{u}$  is the displacement vector and  $\mathbf{U}_{ijk}$  are vectors of displacement approximation coefficients not necessarily associated with nodal displacements, and indexes  $i, j$  and  $k$  in Eq. (3) change from 1 to the total number of approximation functions in each direction. Depending upon the application and geometry, different orders of splines (from 1 to 8) can be used in each direction. Besides changing the order of splines, one can also change their defect (maximum number of discontinuous derivatives) at the node, thus being able to apply standard linear or a higher order p-type finite element approximation if desired. A curvilinear coordinate transformation  $\mathbf{x} = \mathbf{x}(x_1 \ x_2 \ x_3)$ , where  $\mathbf{x}^T = (x, y, z)$ , with Jacobian matrix  $\mathbf{J}(x_1 \ x_2 \ x_3)$  is used to map the unit volume into the global  $x, y, z$ , coordinate system. The Gaussian integration procedure is used to calculate the components of the stiffness matrix.

A critical element of strength prediction in composites with stress concentrations is the modeling of matrix cracking and delaminations precipitating the final failure. An extension of the higher order spline function based displacement approximation (Eq. (3)) to the modeling of

**Fig. 3** Cross sections of the 2.54 mm hole [0/45/–45/90]<sub>s</sub> specimen a small distance from the specimen centerline



displacement field discontinuities occurring in arbitrary directions with respect to the mesh lines was proposed in [7]. This method was applied to multiple matrix crack modeling near an open hole in laminated composites in [8] and [9]. The accuracy of prediction of the redistribution of stress in the fiber direction was verified by using moiré interferometry. In the present paper, multiple cracks and delaminations identified with X-ray images at loads close to failure will be modeled. This mesh independent crack modeling method is based on replacing the true step function, used for element enrichment by Moes et al. [16], by an approximate step function, which is a superposition of the same shape functions used in the displacement approximation (3). Consider a crack or delamination surface  $\Gamma_\alpha$ . To calculate the coefficient of spline approximation for the step function we introduce the signed distance function of the surface  $\Gamma_\alpha$ , which is a scalar function defined for an arbitrary point  $\mathbf{x}$  of the volume. Let  $\bar{\mathbf{x}}$  be the point of the surface  $\Gamma_\alpha$  closest to  $\mathbf{x}$ . Then the signed distance function is given as

$$\chi_\alpha(\mathbf{x}) = \text{sign}[\mathbf{n}(\bar{\mathbf{x}})(\mathbf{x} - \bar{\mathbf{x}})] \|\mathbf{x} - \bar{\mathbf{x}}\|.$$

The surface  $\Gamma_\alpha$  of a crack or delamination is a bounded surface and thereby only for some points  $\mathbf{x}$  the vector  $\mathbf{x} - \bar{\mathbf{x}}$  will be collinear with the normal  $\mathbf{n}(\bar{\mathbf{x}})$ . However, it provides a unique continuous function defined over the entire volume, which changes sign along any path intersecting the surface  $\Gamma$  or its extension. Note that this function is

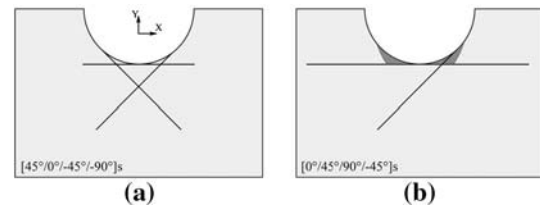


**Fig. 4** Schematics of damage modeled for strength prediction in the (a) [45/0/–45/90]<sub>s</sub> laminate and (b) [0/45/90/–45]<sub>s</sub> laminates

commonly denoted as  $f_\alpha$  which we changed to  $\chi_\alpha$  to avoid confusion with the probability of failure. The coefficients of spline approximation of the step function are then defined as

**Table 2** The length of matrix cracks and the size of delaminations in the final state precipitating fiber failure

| Hole diameter | Matrix crack length and delamination ellipse half axis in (mm) |                                 |
|---------------|--|---------------------------------|
|               | [45/0/–45/90] <sub>s</sub>                                     | [0/45/90/–45] <sub>s</sub>      |
| 2.54 mm       | Splits: $l = 2.54$   | Splits: $l = 7.62$              |
|               | 45 crack $l = 2.54$  | 45 crack $l = 2.54$             |
|               | –45 crack $l = 2.54$   | Delam: $a_x = 1.01, a_y = 1.99$ |
| 6.35 mm       | Splits: $l = 5.08$   | Splits: $l = 7.62$              |
|               | 45 crack $l = 5.08$  | 45 crack $l = 2.54$             |
|               | –45 crack $l = 5.08$   | Delam: $a_x = 2.54, a_y = 3.98$ |
| 12.7 mm       | Splits: $l = 11.6$   | Splits: $l = 11.6$              |
|               | 45 crack $l = 11.6$  | 45 crack $l = 2.54$             |
|               | –45 crack $l = 11.6$   | Delam: $a_x = 5.08, a_y = 7.97$ |

**Table 3** Experimental and predicted values of average failure stress

| Hole diameter | Average experimental and predicted failure loads (MPa) |       |             |                            |       |             |
|---------------|--|-------|-------------|----------------------------|-------|-------------|
|               | [45/0/-45/90] <sub>s</sub>                             |       |             | [0/45/90/-45] <sub>s</sub> |       |             |
| 2.54 mm       | Weibull int.   | 458.3 | (−18.9%)    | Weibull int.               | 465.4 | (−31.2%)    |
|               | CFV  | 589.5 | (+4.2%)     | CFV                        | 679.8 | (0.41%)     |
|               | Experimental   | 565.4 | (c.v. 5.1%) | Experimental               | 677.1 | (c.v. 7.8%) |
| 6.35 mm       | Weibull int.   | 422.2 | (−9.9%)     | Weibull int.               | 407.5 | (−27.3%)    |
|               | CFV  | 474.5 | (+1.2%)     | CFV                        | 561.9 | (0.22%)     |
|               | Experimental   | 468.5 | (c.v. 3.9%) | Experimental               | 560.7 | (c.v. 5.6%) |
| 12.7 mm       | Weibull int.   | 400.6 | (−8.11%)    | Weibull int.               | 436.0 | (−9.0%)     |
|               | CFV  | 432.1 | (−0.8%)     | CFV                        | 476.4 | (−0.5%)     |
|               | Experimental   | 436.0 | (c.v. 9.4%) | Experimental               | 479.2 | (N/A)       |

$$h_i = \frac{\int_V \eta(\chi_\alpha(\mathbf{x}))X_i(\mathbf{x})dV}{\int_V X_i(\mathbf{x})dV}, \tag{4}$$

where the scalar function of a scalar argument  $\eta(\sigma)$  is the Heaviside step function

$$\eta(\sigma) = \begin{cases} 1, \sigma > 0 \\ 0, \sigma \leq 0 \end{cases} \tag{5}$$

The displacement jump step function is approximated as

$$\tilde{H}(\mathbf{x}) = \sum_i h_i X_i(\mathbf{x}), \tag{6}$$

where the three-dimensional spline approximation functions in Eq. (6) are the same as in Eq. (3), i.e.  $X_i(\mathbf{x}) \equiv X_i(x_1)Y_j(x_2)Z_k(x_3)$  for brevity and the single index in the left side runs through all combinations of the three indices in the right side. In the case of a single crack the displacement approximation can be written as

$$\mathbf{u} = \tilde{H}\mathbf{u}^{(1)} + (1 - \tilde{H})\mathbf{u}^{(2)} + \mathbf{u}^{(3)}, \tag{7}$$

where all three displacement approximation functions are approximated according to Eq. (3). The approximation of each displacement functions  $\mathbf{u}^{(m)}$  does not, however contain all shape functions  $X_i(\mathbf{x})$ . The  $\mathbf{u}^{(3)}$  contains only ‘‘far field approximation functions’’ that do not intercept the crack surface at all. The functions  $\mathbf{u}^{(1)}$  and  $\mathbf{u}^{(2)}$  contain the same shape functions, which are the ones intersecting the crack surface. Thus only these shape functions are duplicated and are adding additional degrees of freedom. The linear independence of duplicated shape functions is assured since  $\tilde{H}$  and  $1 - \tilde{H}$  are linearly independent. One could write approximation (7) in the form similar to Eq. (3), where most of the shape functions are the same as in the approximation for the continuous displacement field and a certain number of shape functions, the ones which intersect the crack surface, are duplicated and equal to  $\tilde{H}X_i(\mathbf{x})$  and  $(1 - \tilde{H})X_i(\mathbf{x})$  respectively. These shape

functions, however, may require treatment totally different from that of original shape function  $X_i(\mathbf{x})$ . Indeed, suppose that  $\tilde{H}$  is a true step function jumping on the crack surface, then  $\tilde{H}X_i(\mathbf{x})$  and  $(1 - \tilde{H})X_i(\mathbf{x})$  require new integration domains aligned with the crack surface, which in essence is local remeshing. On the other hand, in the case of the approximate step function (6) the modified shape functions are continuous and have the same support (local area in which they are not equal to zero) as the original function  $X_i(\mathbf{x})$  so that no modification of integration procedures is required at all.

Modeling of multiple cracking configurations is based on consistent application of Eq. (7) to accommodate several surfaces of displacement discontinuity. Depending upon their mutual location one will end up with shape functions such as  $\tilde{H}_1\tilde{H}_2\dots X_i(\mathbf{x})$ , etc. One can easily imagine a configuration in which such a product yields an ill-defined shape function, e.g. multiple cracks crossing in one point. For the problem at hand, however, the main types of interacting cracks are single matrix cracks in a ply and the delamination on the interface, where the resulting shape functions of the product type are well defined.

As mentioned above, two types of displacement discontinuities will be modeled in the parametric studies: ply matrix cracks and delaminations. The surface  $\Gamma_c$  of the ply matrix crack is defined by using four parameters:  $x_0, y_0, \alpha$  and  $l$ , which are the in-plane coordinates of the crack origin, its angle (equal to the ply angle) and length. The crack surface is vertical and spans through the thickness of

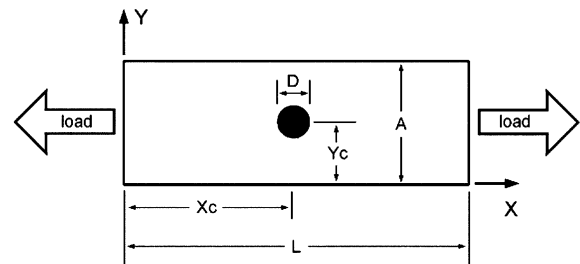


**Fig. 5** Laminated composite with open hole

the ply. The data given in Table 2 define the crack length and angle. The coordinates of the crack origin are calculated simply as

$$x_0 = x_c - l/2, \quad y_0 = y_c \pm D/2$$

in the case of  $0^\circ$  splits. For  $+45$  and  $-45$  ply matrix cracks, they are assumed to originate tangential to the hole, so that

$$x_0 = x_c \mp \frac{D \cos(\pi/4)}{2}, \quad y_0 = y_c \pm \frac{D \sin(\pi/4)}{2}$$

respectively.

The delamination is defined by two user specified functions  $Y_1(x)$  and  $Y_2(x)$  and  $z_0$  (the coordinate of the delaminated plane) so that the delaminated area is bounded by functions  $Y_1$  and  $Y_2$ . The delaminations specified in Table 2 are located on the lower interface of the  $0^\circ$  ply so that  $z_0=3h$ , where  $h$  is the thickness of the ply. Functions  $Y_1(x)$  and  $Y_2(x)$  are defined point wise by pairs of values  $(x, y_1)$  and  $(x, y_2)$  and  $Y_1(x)$  and  $Y_2(x)$  are generated using cubic spline interpolation. The pairs of  $(x,y)$  values are calculated parametrically according to equations

$$\begin{aligned} x &= x_c + a_x \cos(\vartheta), \\ y &= y_c \pm \min(a_y \sin(\vartheta), D/2) \\ 0 &\leq \vartheta \leq \pi, \end{aligned}$$

for 34 uniformly distributed values of  $\vartheta$  and plus and minus signs correspond to  $y_1$  and  $y_2$  respectively.

### Determination of the CFV

In this section we shall discuss the physical meaning of the critical or most likely local failure region in the presence of a stress concentration. We shall consider a Weibull media such that a uniformly loaded sample of given volume has the following probability of failure under stress  $\sigma$ .

$$f(\sigma, V) = 1 - \exp\left(-\frac{V}{V_0} B(\sigma)\right). \quad (8)$$

In the case of a nonuniform stress field Eq. (1) can be generalized in integral form

$$F = 1 - \exp\left(-\frac{1}{V_0} \int_V B(\sigma(\mathbf{x})) dv\right) \quad (9)$$

by applying Eq. (8) to subvolumes of nonoverlapping subdivision and sending their size to zero. In this case the logarithm of total reliability expressed as a sum of loga-

rithms of reliabilities of individual subdomains becomes an integral sum and yields Eq. (9). The implicit assumption made by transitioning from Eq. (8) to Eq. (9) is that the volume scaling given by Weibull distribution is valid in the limit of zero volume. In this context, Eq. (9) expresses the weakest link concept for nonuniformly stressed material and thus provides the probability of failure initiation, i.e. failure of an infinitesimal volume.

We would like to offer a different method of evaluating the probability of failure in a nonuniformly loaded material and set out to estimate the probability of a loss of load carrying capacity (complete failure) of a given subvolume. An algorithm will be proposed to find such a volume, which does not involve a concept of subdivision into mesh cells but instead deals with parametric representation of the nonuniform stress fields. The probability of failure or loss of load carrying capacity was defined so far only for uniformly loaded specimens as their apparent strength, described by distribution function (8). The assumption, which we will use to evaluate the probability of failure in the nonuniformly loaded regions, states that (8) provides a lower bound of probability of failure of a specimen with nonuniform stress distribution, if the stress in each point is higher or equal to  $\sigma$ . Thus the probability of failure  $P$  of a nonuniformly stressed specimen with stress distribution  $\sigma(\mathbf{x})$  can be estimated as

$$P \geq f(\sigma_u, V), \quad (10)$$

if

$$\sigma_u = \min_{\mathbf{x} \in V}(\sigma(\mathbf{x})). \quad (11)$$

The estimate given by Eq. (10) is not very useful when applied to the entire volume of the specimen. On the other hand, one can select a finite region in the nonuniformly loaded specimen, which has a volume  $V_i$  and minimum stress of  $\sigma_i$ , and calculate the probability of failure for this subvolume  $f(\sigma_i, V_i)$ . Suppose that we have found a subregion with volume  $V_c$  and minimum stress  $\sigma_c$ , for which this probability is the highest, i.e.

$$f(\sigma_c, V_c) = \max_i f(\sigma_i, V_i), \quad (12)$$

where index  $i$  scans all subregions of the specimen. Then the subregion  $V_c$  will have the highest probability of local failure, and we will call it CFV.

We shall now describe an algorithm for identification of the CFV and calculation of its failure probability  $f_{\text{CFV}}$ . Denote the magnitude of the maximum stress as  $\sigma_m$ . Introduce a set of iso-stress surfaces  $q_i \sigma_m$ ,  $q_0 = 1 > q_1 > q_2 > q_3 \dots > 0$ . Consider a continuous function  $v(q)$ ,  $0 \leq q \leq 1$ :

$$v(q) = \text{vol}(V_q), \{ \mathbf{x} \in V_q \Leftrightarrow \sigma(\mathbf{x}) \geq q\sigma_m \}. \tag{13}$$

This function is equal to the volume of the specimen with stress higher or equal to  $q\sigma_m$ . The procedure for calculating the overstressed volume function  $v(q)$  is outlined in Appendix 1. The lower bound of the probability of failure for these volumes can be estimated as  $f(q\sigma_m, v(q))$  by using Eq. (8). The latter is a continuous function and its local maximum (if it exists) corresponds to the probability of failure of CFV

$$f_{\text{CFV}} = \max_q f(q\sigma_m, v(q)). \tag{14}$$

Denote by  $q_c$  the value of  $q$  for which  $f_{\text{CFV}} = f(q_c\sigma_m, v(q_c))$  then the respective stress contour  $q_c\sigma_m$  bounds the CFV and its volume will be equal to

$$V_c = v(q_c). \tag{15}$$

The existence of a meaningful value  $0 < q_c < 1$  depends upon both the stress field characteristics as well as that of the material. In the present paper, we will limit ourselves to finite values of  $\sigma_m$ . For an arbitrary stress distribution, which defines the volume function  $v(q)$ , this function can have complex shape. For a typical open hole problem and shape function  $B(\sigma)$  in the form of a two parameter distribution

$$B(\sigma) = \left( \frac{\sigma}{\beta} \right)^\alpha, \tag{16}$$

where  $\alpha$ —is the Weibull modulus or shape parameter and  $\beta$  is an additional constant, one obtains  $f=0$  for  $q=0$  and  $q=1$ . This means that the function  $f(q\sigma_m, v(q))$  will have at least one local maximum ( $f \geq 0$ ) for  $0 < q < 1$ . The fact that  $f=0$  for  $q=1$  follows from the premise that the maximum stress is attained at a point associated with zero volume, i.e.  $v(1)=0$ .

**Physics based limits of CFV**

At the root of the CFV method is identification of the most likely failure region by finding the value  $q_c$  and tracing the region bounded by stress value of  $q_c\sigma_m$  and/or evaluating its volume  $V_c$ . As shown in [15], this capability becomes essential in predicting the fiber failure in composite laminates with stress concentrations. In particular, it was shown that the linear size of CFV defined as

$$l_c = \sqrt{V_c/h},$$

where  $h$  is the thickness of the ply, estimated for quasi-isotropic T300/934 laminates with small 2.54 mm diameter

holes, was significantly below the value of the ineffective length  $\delta$  introduced by Rosen [17]. It is clear that the strength scaling parameters in Eq. (16), which are obtained by testing laboratory size specimens, e.g. [1], are not valid when  $l_c \sim \delta$ . Thus the probability of failure  $f_{\text{CFV}}$  becomes meaningless if  $V_c$  or  $l_c$  is too small. Suppose that one has an estimate of the minimum size volume  $V_{\text{min}}$  for which the Weibull scaling in the form (8) and (16) is valid. In the case of fiber failure, such limits were investigated in [18] by performing Monte-Carlo simulation of failure of square cross sections of fiber bundles of three different length  $3\delta$ ,  $6\delta$  and  $9\delta$ . A value of  $l_{\text{min}} = 6\delta$  was considered the minimum scalable length in their study for fibers with Weibull modulus in the range of 10. Although this is higher than the values of 5–6 for typical carbon fibers it can be used to estimate  $V_{\text{min}}$  as

$$V_{\text{min}} = l_{\text{min}}^2 h. \tag{17}$$

Having a value of  $V_{\text{min}}$  one can a priori evaluate the validity of a  $f_{\text{CFV}}$  prediction comparing  $V_c$  and  $V_{\text{min}}$ . However, more importantly if  $V_c$  and the value of  $f_{\text{CFV}}$  is physically inadmissible, one can simply obtain another physically admissible estimate of the probability of failure by finding the maximum local probability of failure of only those subvolumes which are larger or equal to  $V_{\text{min}}$ . In other words we will replace the definition of CFV given by Eq. (14) by slightly modified one

$$f_{\text{CFV}} = \max_{v(q) \geq V_{\text{min}}} f(q\sigma_m, v(q)). \tag{18}$$

The practical calculation of a new value of  $q$ , say  $q_0$ , such that  $f_{\text{CFV}} = f(q_0\sigma_m, v(q_0))$  satisfies Eq. (18) is also straight forward at least in the case when  $V_{\text{min}}$  and  $V_c$  are both much smaller than the specimen volume. In this case  $q_0$  is simply calculated by solving the equation  $v(q_0) = V_{\text{min}}$ . Indeed if  $q_c$  provides an absolute maximum for the function  $f(q\sigma_m, v(q))$  then the conditional maximum, such that  $v(q) \geq V_{\text{min}}$  will take place at  $q = q_0$  as long as the function  $f(q\sigma_m, v(q))$  is monotonic on the interval  $q_0 \leq q \leq q_c$ .

It might appear that the correction for the minimum scalable volume is an issue pertaining to the CFV method. On the contrary, this is a problem related to material heterogeneity and stress concentration in any volumes in which size becomes comparable to the scale of the microstructure. It will be shown below that the Weibull integral calculated in problems when the application of the CFV method yields  $V_c < V_{\text{min}}$  gives unacceptably conservative strength values due to the fact that most of the contribution to the Weibull integral comes from the very region  $V_c$ . However, due to its integral nature there are no simple modifications to solve this problem. The solution proposed by Bazant in the 90’s and known as nonlocal



Weibull theory [19] proposes to first calculate stress averages over certain physically dictated characteristic volumes such as  $V_{\min}$  and then use these averages in the secondary integration of the Weibull integral. Such approach clearly addresses the problem at hand, but requires considerably more effort for practical implementation.

## Results and discussion

In this section we will discuss the results of strength prediction of the two quasi-isotropic laminates considered in the experimental section by using the CFV method defined by Eq. (18) and the standard Weibull integral method (9). The value of  $V_{\min}$  in the CFV method is calculated by using Eq. (17) and thus depends upon the ply thickness. Therefore the minimum scalable volume as such is not a material parameter at all and will be used for intermediate purposes of calculating  $q_0$ . The minimum length  $l_{\min}$  has, however, a very clear physical meaning: it is the width of the process zone of formation of a crack in the direction perpendicular to fiber orientation. In [15] this value was taken to be equal to  $l_{\min}=6\delta$ , where the ineffective length  $\delta$  is computed according to Rosen [17]:

$$\delta = 1.14d_f \sqrt{\frac{1}{\sqrt{v_f}} - 1} \sqrt{\frac{E_f}{G_m}}, \quad (19)$$

where  $d_f$  and  $E_f$  are the diameter and the Young's modulus of the fiber,  $G_m$  is the matrix shear modulus and  $v_f$  is the fiber volume fraction. The multiplier 6, which is the single parameter postulated in the present analysis, has some justification based on recent results of Landis et al. [18] and is in the range of data generated by half a century of research following the cited paper by Rosen. The IM7 fiber and 5250-4 matrix properties given by Pagano et al. [20] were used to obtain a value of  $l_{\min} = 0.266$  mm at  $v_f = 60\%$ , which will be used for strength prediction below. Note that the value used in [15] for the T300/934 material system was  $l_{\min} = 0.323$  mm mostly due to a different fiber diameter and showed a good agreement with archival open hole strength data for that system. The ply stiffness parameters for IM7/5250-4 were as follows:  $E_{11}=166.6$  Gpa,  $E_{22} = E_{33} = 9.44$  Gpa,  $\nu_{13} = \nu_{13} = 0.33$ ,  $\nu_{23} = 0.58$ ,  $G_{12} = G_{13} = 6.06$  Gpa and  $G_{23} = 2.96$  Gpa. The Weibull parameters for the strength in the fiber direction are those from [11] and equal to  $X_t = 2.41$  Gpa,  $V_0 = 38,400$  mm<sup>3</sup> and  $\alpha = 40$ .

The average strength values predicted for the two laminates with three hole sizes both by using the CFV and the Weibull integral methods are shown in Table 3, which also contains the experimental results. The average value of strength in all cases was calculated based on probability of

failure as described in Appendix 2. The values in parenthesis next to the average values refer to different things for theoretical and experimental data. For the experimental data they show the coefficient of variation (standard deviation divided by the average value) in percent. In the case of predicted values they denote the deviation from the average strength obtained experimentally, i.e. (prediction-test data)/test data\*100%. All predictions were made by applying the statistical criteria to stress fields resulting from modeling the damage given in Table 2.

In the case of the large 12.7 mm hole in the [45/0/-45/90]<sub>s</sub> laminate, the value of strength predicted by CFV method and Weibull integral are within one standard deviation from the experimental average value. Indeed, the deviation shown in parentheses is less than the coefficient of variation of the experimental data. Decreasing the hole size, however, leads to divergence between the predictions by the two methods. The CFV predictions stay within one standard deviation from test data in all cases while the Weibull integral method underpredicts the strength by as much as 16–19% for the smaller hole sizes. This result can be explained by calculating the  $l_c$  predicted by the CFV method, which in the case of the 6.35 and 2.54 mm are 0.0528 mm and 0.0252 mm, respectively. These values are significantly smaller than  $l_{\min}=0.266$  mm and even  $\delta=0.044$  mm, which indicates that contribution to Weibull integral coming from such small volume is inaccurate.

In the case of the stronger laminate [0/45/90/-45]<sub>s</sub> the same trend, amplified by the effect of damage, is present as well, although the Weibull integral method is even more significantly underpredicting the experimental values. Table 4 displays the results of ultimate strength prediction for the two laminates with 6.35 mm hole based on stress fields predicted for different extents of damage. The columns left to right show the predicted strength based on 0° ply stress distribution calculated without any matrix damage present, with splitting in the 0° ply only, with splitting and delamination (not present for the weak laminate) and with the final damage state as given in Table 2. The numbers in parenthesis are the deviations from the experimental values of 468.5 Mpa and 560.7 Mpa, respectively. In the case of the weaker laminate the Weibull integral based prediction jumps from -22% to -10% below the experimental data due to stress relaxation as a result of splitting. Further introduction of the 45° cracks practically does not change the prediction. The CFV method predicts different values of strength based on exactly the same stress distributions. It in fact predicts a much smaller effect of stress redistribution on the ultimate strength. Even the strength predicted without taking into account any damage is within one standard deviation from the experimental value. The introduction of damage increases the predicted

**Table 4** Average strength values predicted for different extent of matrix damage in specimens with 6.35 mm hole diameter

| Laminate                   |              | Average predicted strength (Mpa) and deviation from test % |              |                  |             |
|----------------------------|--------------|--|--------------|------------------|-------------|
|                            |              | No damage  | Splits       | Splits and delam | All damage  |
| [45/0/-45/90] <sub>s</sub> | Weibull int. | 362.3 (-22)  | 419.9 (-10)  |                  | 422.5 (-10) |
|                            | CFV          | 454.3 (-3.0)   | 470.9 (-0.5) |                  | 474.5 (1.2) |
| [0/45/90/-45] <sub>s</sub> | Weibull int. | 346.4 (-38)  | 411.4 (-26)  | 499.8 (-11)      | 407.8 (-27) |
|                            | CFV          | 452.0 (-19)  | 499.2 (-11)  | 546.0 (-2.6)     | 562.9 (0.2) |

strength, however the total range of deviation from test data is -3% to 1.2%.

In the case of the laminate with the outer 0° plies the effect of damage on the predicted strength is much more pronounced. Sequential addition of splitting and delamination brings the prediction by both methods closer to experimental data. However, the addition of the 45° crack causes an unexpected reduction of the ultimate strength prediction by using the Weibull integral method, where as the CFV result changes only slightly and in the opposite direction. Such behavior of the Weibull integral based prediction at first seems to contradict the observation for the first laminate. This effect can be explained by examining the stress distributions in the 0° ply of the [0/45/90/-45]<sub>s</sub> laminate, which are predicted in the presence of only splitting and delamination, Fig. 6a, and in the presence of all damage, Fig. 6b. It appears that a small area of high

fiber direction stress is developing near the intersection of the splits and 45° cracks, whereas the stress concentration near the hole edge is approximately the same in the two cases. The experimental evidence of such stress concentration was reported in [9]. The drop of predicted strength values by Weibull integral can be explained by its sensitivity to overstress even in a very small volume due to the very high value of the Weibull modulus  $\alpha=40$ . The CFV method is much less sensitive to point values of high stress because of the minimum length parameter  $l_{min}$ . A similar phenomenon is happening in the first laminate. The final strength predicted for the [0/45/90/-45]<sub>s</sub> laminate by using Weibull integral was 422.5 Mpa which is very close to that predicted by the same method for the second laminate 407.4 Mpa. These predictions are defined by the stress concentration developing due to the interaction of the 45° ply cracks with splits in the 0° ply.

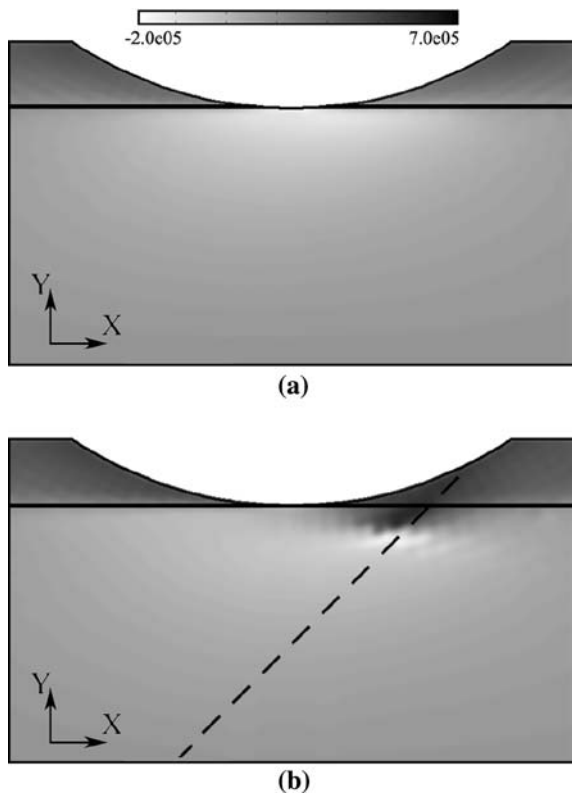


**Fig. 6** Axial stress distribution in the 0° ply near the hole edge in the presence of damage, (a) splitting and delamination and (b) splitting, delamination and one 45° crack

**Conclusions**

An experimental study of tensile strength of two carbon fiber quasi-isotropic laminates with stacking sequences [45/0/-45/90]<sub>s</sub> and [0/45/90/-45]<sub>s</sub> was performed for three hole sizes. The first laminate showed 20% lower strength for smaller and 10% lower for the larger hole sizes. X-radiography and sectioning studies were performed to evaluate the state of matrix damage precipitating fiber failure. No delaminations were observed for the first laminate and only small delamination, not in the high stress concentration area, were observed in the [0/45/90/-45]<sub>s</sub> laminate. The length of the splitting of the 0° ply and cracking in the 45° plies neighboring with the 0° ply were tabulated along with the extent of delamination.

A mesh-independent crack modeling method based on approximation of the Heaviside step function by using higher order shape functions was used to model the effect of multiple damage on stress distribution in both laminates under consideration. Fully three-dimensional analyses were employed with quadratic approximation of displacement through the thickness of each ply.

CFV method with a minimum scaling length (volume) constraint was employed for failure prediction in the two laminates along with the traditional Weibull integral method. The strength prediction was based on the state of

stress in the  $0^\circ$  ply resulting from stress redistribution due to matrix damage in the form of splitting, delamination and matrix cracking of the neighboring plies. The CFV method gave results within one standard deviation from experimentally observed strength values for both laminates and all three hole sizes. The Weibull integral methods under-predicted the strength in all cases from as much as 20–30% for smaller hole sizes to 8% for the large holes. Such large disagreement was explained by the high sensitivity of the Weibull integral predictions to high stress concentrations over even very small areas because of the high value of the Weibull modulus  $\alpha = 40$ , which was used in the analysis.

The accuracy of the failure prediction by using CFV is attributed to the introduction of the minimum scaling length (volume) parameter, which limits the size of the volume to which Weibull scaling is applied. Such a limit has clear physical explanation in the case of fiber failure, which is a process involving accumulation and interaction of single fiber breaks developing over a band of several ineffective lengths wide. The width of this band is the minimum scalable length,  $l_{\min}$ . A direct measurement or rigorous evaluation of this parameter is, however, difficult. Consistent with sited micromechanical studies, its value was assigned equal to six times the Rosen's ineffective length.

**Acknowledgements** The work was supported by Air Force Research Laboratory through contract number FA8650-05-D-5052 to the University of Dayton Research Institute. The authors are grateful to Chase Nessler of the Southwest Council of Higher Education for performing the sectioning studies.

## Appendix 1

### Computation of the $v(q)$ function

After the solution is completed and all vectors  $\mathbf{U}_{ijk}$  are determined, a post-processing step is performed in which each integration point of the structure is examined twice. First the stress and strain components are computed, and the maximum value  $\sigma_m$  of the component of interest is found by searching through all integration points. A large number  $M$  (in our analysis  $M = 101$  and  $201$ ) is then prescribed, and a sequence

$$q_i = 1 - i/M, \quad i = 0, \dots, M,$$

defined. The overstressed volume function  $v(q)$  is then calculated in  $M$  points as

$$v(q_i) = \sum_{g_1} \sum_{g_2} \sum_{g_3} w_{g_1} w_{g_2} w_{g_3} \det J(x_1^{g_1}, x_2^{g_2}, x_3^{g_3}) \eta(\sigma - q_i \sigma_m) \quad (20)$$

In Eq. (20) indexes  $g_i$ ,  $i=1,2,3$  denote Gauss integration points in  $x_1$ ,  $x_2$  and  $x_3$  directions, respectively, and  $w_{g_i}$  are respective Gaussian weights. Heaviside step function (5) cuts off the contribution from all integration points where the stress is lower than the threshold  $q_i \sigma_m$ . For low values of the threshold value,  $v(q)$  will include almost all integration points in (20) and become close to the entire volume.

## Appendix 2

### Average strength value calculation

For Weibull distribution (8) with shape function (16), the average value of strength  $\sigma_a$  and the coefficient of variation  $\omega$  (standard variation divided by average value) are given by well known equations:

$$\sigma_a = \beta \left( \frac{V_0}{V} \right)^{1/\alpha} \Gamma \left( 1 + \frac{1}{\alpha} \right), \quad (21a)$$

$$\omega = \sqrt{\frac{\Gamma(1 + 2/\alpha)}{\Gamma^2(1 + 1/\alpha)}} - 1, \quad (21b)$$

where  $\Gamma$ -denotes the gamma function. By using Eq. (21a), one can find the average strength value for a known  $\alpha$  if the probability of failure is known for just for one value of  $\sigma$ , i.e.  $f$  is equal to  $f_1$  for  $\sigma = \sigma_1$ . In this case

$$\sigma_a = \sigma_1 (-\ln(1 - f_1))^{-1/\alpha} \Gamma \left( 1 + \frac{1}{\alpha} \right) \quad (22)$$

Equation (22) will be used to calculate the average strength for both the Weibull integral and CFV method based estimates of the probability of failure.

## References

1. ASTM D3039/D3039M-00e2. Standard test method for tensile properties of polymer matrix composites. ASTM International, West Conshohocken, PA, December, 2000
2. Whitney JM, Nuismer RJ (1974) J Compos Mater 8:253
3. Waddoups ME, Eisenmann J and Kaminski BE (1971) J Compos Mater 5:446
4. Nuismer RJ, Whitney JM (1975) Fract Mech Compos, ASTM STP 593:117
5. Whitney JM, Kim RY (1976) Effect of stacking sequence on the notched strength of laminated composites, AFML-TR-76-177
6. Kortshot MT, Beaumont PWR (1990) Compos Sci Technol 39:303
7. Iarve EV (2003) Int J Mth Eng 56:869
8. Iarve EV, Mollenhauer DH, Kim R (2005) Compos Part A 36:163
9. Mollenhauer D, Iarve EV, Kim R, Langley B (2006) Composites: Part A 282:294
10. Wismon MR (1999) Compos Sci Technol 59:1937

11. Wisnom MR, Khan B, Green B, Jiang W, Hallet SR (2005) Specimen size effects on tensile strength and failure mechanisms of carbon/epoxy composites. JNC14 Conference, Compiègne, March 2005
12. Wu EM (1978) Failure analysis of composites with stress gradients, UCRL-80909
13. Wetherhold RC and Whitney JM (1981) *Polymer Compos* 2(3):112
14. Wetherhold RC (1985) *J Compos Mater* 19:19
15. Iarve EV, Mollenhauer DH, Kim R (2006) *Composites Part A* (accepted)
16. Moes N, Dolbow J and Belytschko T (1999) *Int J Numer Methods Eng* 46:131
17. Rosen BW (1964) *AIAA J* 2:1985
18. Landis CM, Beyerlin IJ, McMeeking RM (2000) *Mech Phys Solids* 48:621
19. Bazant ZP (2002) *Scaling of structural strength*. Hermes Penton Science (Kogan Page Science), London
20. Pagano NJ, Schoeppner GA, Kim R, Abrams FL (1998) *Compos Sci Technol* 58:1811